MODELING REACTING MULTI-SPECIES FLOWS WITH A DETAILED MULTI-FLUID LATTICE BOLTZMANN SCHEME

by

Chao NING*, Shouqi YUAN, Jinfeng ZHANG, and Yalin LI

National Research Center of Pump, Jiangsu University, Zhenjiang, Jiangsu, China

Original scientific paper
https://doi.org/10.2298/TSCI190626140N

Recent advances and findings reported in the literature show that the lattice Boltzmann method can be a viable and rather efficient alternative to classical numerical methods in modeling multi-species flows. Based on the kinetic theory of multicomponent gases, multi-fluid approaches are derived. Each species evolves according to the specific properties, a proper coupling must be introduced for modeling the diffusivity. In recent years, a discrete kinetic scheme for multi-component flows has been proposed which was able to solve the Maxwell-Stefan system of equations for any number of species. However, reacting flows lead to additional challenges and have seldom been studied by lattice Boltzmann method. The aim of the present work is to implement this model in the lattice Boltzmann solver, extend it to take account multiple chemical reactions. The temperature is modeled through separate distribution function and the flow distribution function is assumed to be independent of temperature. The performance has been checked for a binary diffusion flow and a counter-current propane/air reacting flow. The obtained results show that this model able to deal with multi-species flows and solves the multi-component system of equations

Key words: *lattice Boltzmann, multi-species flows, multi-component models, reacting flows*

Introduction

With two decades' development, the lattice Boltzmann (LB) method has been gradually accepted as a useful alternative to simulate various complex fluid systems [1]. The popularity of this method is based in part on its simple formulation and application to flow problems compared with solving the Navier-Stokes (N-S) equations, and in part on the high level of scalability on parallel processing systems [2]. So far, the mostly used model equation for the Boltzmann formulation is the Bhatnager-Gross-Krook (BGK) equation, named after those who first proposed it, Bhatnager *et al.* [3]. They noticed that the main effect of the collision term is to bring the velocity distribution function closer to the equilibrium distribution. The Lattice Boltzmann BGK method (LBBGK) is a numerical scheme for simulating viscous compressible flows in the subsonic regime [4, 5]. In recent years, LBGK has achieved great success in simulations of fluid flows and in modeling physics in fluids.

Given the complex nature of multi-species flows and the associated computational costs, it is important to develop computationally efficient solvers for them. Different models have been developed in the context of LB for different levels of physical approximations,

* Corresponding author, e-mail: dream0830@163.com

from the generalized Fick model to more complex models such as the Maxwell-Stefan system of equations. In the modelling of mixtures of gases, the effect of the different molecular masses of the gases must be taken into consideration and the collision term must be modified to take account the momentum exchanged between the species. Gunstensen *et al.* [6] introduced a color gradient model. Two components represent two types of fluid with their own distribution functions, and follow their own evolution equation. The collision step includes self- and cross-interactions with other types of particles. Orlandini *et al.* [7], Osborn *et al.* [8], and Swift *et al.* [9] developed the free energy model. This model included thermodynamic equilibrium functions of phases and a term describing the surface tension was added to the equilibrium distribution function. It is a fully thermodynamically consistent binary fluid LB model. Sofonea and Sekerka [10] who realized that if BGK-style models were used to describe the collision process, adopted the approach with functions of the self-collision and cross-collision relaxation frequencies. In the approach of [11, 12], an LB model for low Mach number flows with variable density, is developed based on a LBBGK model. An advanced BGK model proposed by Andries *et al.* [13] in case of isothermal flow, which is based on only one global operator for each species. Based on Sirovich's theory [14], Luo [15] developed a unified approach for developing the LB models for multicomponent fluids. The model in [16] have adopted a force coupling in the momentum equations, derived from a linearized kinetic term and further the model by Asinar [17, 18] avoided a linearization by two collision operators. In [19] another LB scheme has been proposed aiming to minimize a proper H function defined on the fully discrete lattice. Flekkoy [20] and Shan and Chen [21, 22] developed a pseudopotential LB model, this model properly takes account the momentum exchange between the species by pseudopotential interactions. The thermal pseudopotential LB method was firstly attributed by Zhang and Chan [23], then Li *et al.* [24] developed a hybrid thermal LB-MRT model considering the vapor-liquid phase change and this model was extended to the multicomponent LB model by Zheng *et al.* [25, 26]. The models introduced above have been well studied by many authors, however, these models have various shortcomings. Some of them work only for binary mixtures, others resolve only Fick's diffusion instead of Maxwell-Stefan diffusion and others are not parameter free. In [27] the authors presented a LB method, consisted with gas and liquid multicomponent flows, which remedied these shortcomings.

The present work implements the model by Zudrop *et al.* [27] in the LB solver, extend it to take account multiple chemical reactions. This model will be implemented in our in-house code ALBORZ [28, 29] and benchmarked for a variety of configurations in this framework. The obtained performance and scalability maintain the computational advantages of the standard LB method.

Lattice Boltzmann equations

The Boltzmann transport can be written:

$$\frac{\partial f}{\partial t} + \vec{\xi}\vec{\nabla} f + \frac{\vec{\mathrm{F}}}{m}\vec{\nabla}_{\vec{\xi}} f = \Omega \tag{1}$$

Equation (1) is an advection equation with a source term Ω, or advection with a reaction term, which can be solved exactly along the characteristic lines that is tangent to the vector $\vec{\xi}$, if Ω is explicitly known. With a BGK relaxation term ω and the local equilibrium distribution function $f^{(\mathrm{eq})}$, the collision operator is replaced:

$$\Omega = \omega[f^{(\mathrm{eq})} - f] = \frac{1}{\tau}[f^{(\mathrm{eq})} - f] \tag{2}$$

where ω is the collision frequency and $\tau = 1/\omega$ – the relaxation factor. Physically, the approximation captures the relaxation due to intermolecular collisions of a non-equilibrium gas, f, towards its equilibrium distribution function, $f^{(\mathrm{eq})}$. This explains the appearance of the collision frequency, the higher the frequency of collisions, the more rapid the convergence to equilibrium. After BGK approximation, the collision operator is now linearized, the Boltzmann equation (without external forces) can be approximated:

$$\frac{\partial f}{\partial t} + \vec{\xi}\vec{\nabla} f = \frac{1}{\tau}[f^{(\mathrm{eq})} - f] \tag{3}$$

In LB method, the previous equation is discretized and assumed it is valid along specific directions, the solution domain is divided into lattices:

$$\frac{\partial f_\alpha}{\partial t} + \vec{c}_\alpha \vec{\nabla} f_\alpha = \frac{1}{\tau}[f_\alpha^{(\mathrm{eq})}(x,t) - f_\alpha(x,t)] \tag{4}$$

At each lattice node, the factitious particles reside. Some of these particle streams along specified directions to the neighboring nodes. The number of directions, linkage, depends on the lattice arrangement. The common terminology used in LB methodis to refer to the dimension of the problem and the number of speeds is using D_nQ_m, where n represent the dimension of the problem and m refers to the speed model, number of linkages. The velocity directions of the D_2Q_9 LBGK model are defined:

$$e_i = \begin{cases} (0,0) & i = 0 \\ \cos\left[(i-1)\dfrac{\pi}{2}\right], \quad sin\left[(i-1)\dfrac{\pi}{2}\right]c & i = 1,2,3,4 \\ \sqrt{2}\cos\left[(i-1)\dfrac{\pi}{2} + \dfrac{\pi}{4}\right], \quad sin\left[(i-1)\dfrac{\pi}{2} + \dfrac{\pi}{4}\right]c & i = 5,6,7,8 \end{cases} \tag{5}$$

where $c = \delta_x/\delta_t$ and δ_x and δ_t are the lattice constant and the time step size, respectively. In order to recover the N-S and continuity equations, the equilibrium distribution function is set to:

$$f_\alpha^{(\mathrm{eq})} = \rho\omega_\alpha\left[1 + 3\frac{(\vec{e}_\alpha\vec{u})}{c^2} + \frac{9}{2}\frac{(\vec{e}_\alpha\vec{u})^2}{c^4} - \frac{3}{2}\frac{\vec{u}^2}{c^2}\right] \tag{6}$$

with the weight coefficient:

$$w_\alpha = \begin{cases} \dfrac{4}{9} & \alpha = 0 \\ \dfrac{1}{9} & \alpha = 1,2,3,4 \\ \dfrac{1}{36} & \alpha = 5,6,7,8 \end{cases} \tag{7}$$

The fluid density, ρ, and velocity, $\vec{u}$, are obtained from the density distribution function $f_\alpha(x, t)$:

$$\rho = \sum_{\alpha} f_{\alpha} \tag{8}$$

$$\rho\vec{\mathrm{u}} = \sum_{\alpha} \vec{\mathrm{e}}_{\alpha} f_{\alpha} \tag{9}$$

The mass and momentum equations can be derived from the model *via* multiscaling expansion:

$$\frac{\partial \rho}{\partial t} + \vec{\nabla}(\rho\vec{\mathrm{u}}) = 0 \tag{10}$$

$$\frac{\partial \rho\vec{\mathrm{u}}}{\partial t} + \vec{\nabla}(\rho\vec{\mathrm{u}}\vec{\mathrm{u}}) = -\vec{\nabla}p + \nu\left\{\vec{\nabla}^2(\rho\vec{\mathrm{u}}) + \vec{\nabla}[\vec{\nabla}(\rho\vec{\mathrm{u}})]\right\} \tag{11}$$

where $p = c_s^2\rho$ is the pressure $c_s = c/\sqrt{3},$ is the sound speed, and $\nu = (2\tau - 1)c^2\delta t/6$ is the kinematic viscosity.

Model for species diffusion

Diffusion describes the spreading of particles through random motion usually from regions of higher concentration to regions of lower concentration. The diffusion velocity is the term describing the bet flux due to this random motion. The diffusion velocities can be computed through the Maxwell-Stefan system of equations:

$$\vec{\nabla}X_p = \sum_{p=1}^{N} \frac{X_k X_p}{D_{pk}(V_p - V_k)} + (Y_p - X_p)\frac{\vec{\nabla}P}{P} + \frac{\rho}{P}\sum_{p=1}^{N} Y_p Y_k (f_p - f_k) +$$

$$+\sum_{p=1}^{N}\left[\left(\frac{X_k X_p}{\rho D_{pk}}\right)\left(\frac{D_{T,k}}{Y_k} - \frac{D_{T,p}}{Y_p}\right)\right]\left(\frac{\vec{\nabla}T}{T}\right) \qquad \text{for} \quad p = 1, N \tag{12}$$

where $D_{pk} = D_{kp}$ is the binary mass diffusion coefficient of species p into species k. The $D_{T.k}$ is the thermal diffusion coefficient for species k. The mole fraction of k^{th} species X_k is computed:

$$X_k = Y_k \frac{W}{W_k} \tag{13}$$

with W is the mean molecular weight of the mixture and W_k – the molecular weight of species k. The mass fraction Y_k for k = 1 to N where N is the number of species in reacting mixture. Y_k is defined by:

$$Y_k = \frac{m_k}{m} \tag{14}$$

where m_k is the mass of species k and m – the total mass of gas in this volume. Neglecting higher order effects, such as thermal diffusion, pressure diffusion and body forces, the Maxwell-Stefan equation for N species can be re-written:

$$\vec{\nabla}X_p = \sum_{p=1}^{N} \frac{X_k X_p}{D_{pk}(V_p - V_k)} \tag{15}$$

Note that the concentration gradient of species k depends on the difference in velocity of the k^{th} species and all the other species in the mixture.

Flow field

The total mass and momentum conservation equations are modeled for fluid dynamics by [30]:

$$\frac{\partial \rho}{\partial t} + \frac{\partial \rho \vec{\mathrm{u}}_i}{\partial x_i} = 0 \tag{16}$$

$$\rho \frac{\partial \vec{\mathrm{u}}_j}{\partial t} + \rho \vec{\mathrm{u}}_j \frac{\partial \vec{\mathrm{u}}_i}{\partial x_i} = -\frac{\partial p}{\partial x_j} + \frac{\partial}{\partial x_i}\left(\mu \frac{\partial \vec{\mathrm{u}}_i}{\partial x_i}\right) + \rho \sum_{k=1}^{N} Y_k f_{k,j} \tag{17}$$

In eq. (17), $f_{k,j}$ is the volume force acting on species k in direction j. The mass conservation equation for species k is written:

$$\frac{\partial \rho Y_k}{\partial t} + \frac{\partial}{\partial x_i}[\rho(\vec{\mathrm{u}}_i + V_{k,i})Y_k] = \dot{\omega}_k \qquad \text{for} \quad k = 1, N \tag{18}$$

In eq. (18), $V_{k,i}$ is the i^{th} component of the diffusion velocity V_k of species k and $\dot{\omega}_k$ is the reaction rate of species k:

$$\sum_{k=1}^{N} Y_k V_{k,i} = 0 \tag{19}$$

$$\sum_{k=1}^{N} \dot{\omega}_k = 0 \tag{20}$$

To extend the LB method to multicomponent flows, the interaction of the species has to be taken into account, which is usually achieved by a modification of the equilibrium part and the relaxation towards it. The LB model derived in [27] presented a finite discrete velocity model:

$$\partial_t f_k^m + \vec{\mathrm{u}}^m \vec{\nabla} f_k^m = \lambda_k (f_k^{(\mathrm{eq}),m} - f_k^m) \tag{21}$$

where the relaxation parameter λ_k for species k is defined by:

$$\lambda_k = \frac{KB}{\rho} \tag{22}$$

where K is the bulk modulus of the mixture and B is a free parameter to be chosen with respect to stability. In particular, we obtain $c_s^2 = K/\rho$ and this model assigned the same relaxation parameter to all the species, we choose $B = 6$ such that $\lambda_k = 2$. After applying a reformulation in terms of the transformed variable $\bar{f}_k^m = f_k^m + \lambda_k \delta_t / 2[f_k^m - f_k^{(\mathrm{eq}),m}]$. The LB method like scheme:

$$\bar{f}_k^m(x + \vec{\mathrm{u}}^m \delta_t, t + \delta_t) = \bar{f}_k^m(x,t) + \frac{\delta_t}{\dfrac{1}{\lambda_k} + \dfrac{\delta_t}{2}}[f_k^{(\mathrm{eq}),m}(x,t) - \bar{f}_k^m(x,t)] \tag{23}$$

The equilibrium of the model is given by:

$$f_k^{(\mathrm{eq}),m} = \omega^m \rho_k \left[s_k^m + \frac{\vec{\mathrm{u}}^m \vec{\mathrm{v}}_k^*}{c_s^2} + \frac{(\vec{\mathrm{u}}^m \vec{\mathrm{v}})^2}{c_s^4} - \frac{\vec{\mathrm{v}}^2}{2c_s^2} \right] \tag{24}$$

where ω^m are the lattice weights. A modified velocity $\vec{\mathrm{v}}_k^*$ for each species k in the bilinear equilibrium part is defined:

$$\vec{\mathrm{v}}_k^* = \vec{\mathrm{v}}_k + \sum_l \frac{B_{k,l}}{B} \phi_k \chi_l (\vec{\mathrm{v}}_l - \vec{\mathrm{v}}_k) \tag{25}$$

and mass averaged mixture velocity $\vec{\mathrm{v}}$ in the equilibrium part is defined:

$$\vec{\mathrm{v}} = \sum_l \frac{\rho_l \vec{\mathrm{v}}_l}{\rho} \tag{26}$$

The mass averaged mixture velocity $\vec{\mathrm{v}}$ recovers Maxwell-Stefan diffusion equations for each species k. According to the applied variable transformation, the modified mixture velocity $\vec{\mathrm{v}}_k^*$ can be computed for $t + \delta_t$ by solving anelement local linear equation system for $\vec{\mathrm{v}}_k$ and plugging it in eq. (25):

$$\vec{\mathrm{v}}_k^* = \vec{\mathrm{v}}_k + \frac{\delta_t \lambda_k}{2} \sum_l \frac{B_{k,l}}{B} \phi_k \chi_l \vec{\mathrm{v}}_k - \frac{\delta_t \lambda_k}{2} \frac{1}{\rho_k} \sum_l \frac{B_{k,l}}{B} \phi_l \chi_k \rho_l \vec{\mathrm{v}}_l \tag{27}$$

Hence, the scheme remains fully explicit. The parameters in eq. (24) for a D_2Q_9 lattice are defined:

$$\begin{aligned} \phi_k &= \frac{min_\alpha m_\alpha}{m_k}, \qquad B_{k,l} = \frac{1}{D_{k,l}} \\ s_k^m &= \begin{cases} \dfrac{9 - 5\phi_k}{4} & \text{if} \quad m = 0 \\ \phi_k & \text{else} \end{cases} \end{aligned} \tag{28}$$

where $min_\alpha m_\alpha$ is the minimal molecular weight of all species. Macroscopic quantities are obtained as moments of f_k^m, density $\rho_k = \Sigma_m f_k^m$ and velocity $\vec{\mathrm{v}}_k = \Sigma_m \vec{\mathrm{u}}^m f_k^m$.

Temperature field

The passive scalar approach consists of solving an additional transport equation for the scalar being modeled. In this section, temperature is modeled through an advection-diffusion LB scheme shown to recover the following PDE:

$$\frac{\partial T}{\partial t} + \vec{\mathrm{u}}_i \frac{\partial T}{\partial x_i} = \frac{\partial}{\partial x_i} \left(\frac{\lambda}{c_{p0} \rho_0} \frac{\partial T}{\partial x_i} \right) - \sum_{k=1}^{K} W_k \dot{\omega}_k h_k \tag{29}$$

The distribution function for the temperature field is:

$$g^m(x + u^m \delta_t, t + \delta_t) = g^m(x,t) - \frac{1}{\tau_\mathrm{T}} [g^{(\mathrm{eq}),m}(x,t) - g^m(x,t)] + \omega^m \frac{\omega_{\mathrm{ov}} \dot{Q} \delta_t}{\rho C_p} \tag{30}$$

where C_p [Jkg^{-1}K^{-1}] is the heat capacity and it is often assumed to be constant in many theoretical approaches and combustion codes, $\dot{Q}$ [Jmol^{-1}] is the heat of overall reaction, and

ω_{ov} [kgm^{-3}s^{-1}] – the overall reaction rate. The relaxation coefficients of temperature scheme can be related to thermal diffusivity, k, given by:

$$\kappa = \frac{2\tau_T - 1}{6} c^2 \delta_t \tag{31}$$

The temperature T is calculated by $T = \Sigma_m g^m$, the corresponding LB time-evolution algorithm is:

$$g^{(eq),m} = \omega^m T \left[1 + 3\frac{\vec{u}^m \vec{v}}{c_s^2} + 9\frac{(\vec{u}^m \vec{v})^2}{c_s^4} - 3\frac{\vec{v}^2}{2c_s^2} \right] \tag{32}$$

Computational set-up

In order to have a better idea of the possible sources of error in weakly-compressible LB-type numerical algorithm, the multi-component algorithm is benchmarked through text-cases ranging from a binary diffusion configuration, with species having the same molar mass and different molar masses, to a counter-current propane/air reacting flow [31].

Case 1. Binary diffusion flow

The first simulation set-up, taken from [32], consists of two chemical species with the same molar mass. The binary diffusion coefficient, $D_{\sigma\varsigma}$, is defined to be 0.68 cm^2/s, The computational domain has 500 lattice nodes in the y-direction with periodic boundary conditions on the horizontal boundaries and bounce-back boundary conditions on the vertical boundaries. The overall configuration is shown in fig. 1. The lattice parameters have the following values: δ_x = 3.85 um and δ_t = 44 ns. The initial density profile for each species is assumed to have a hyperbolic tangent profile in the y-direction of the form:

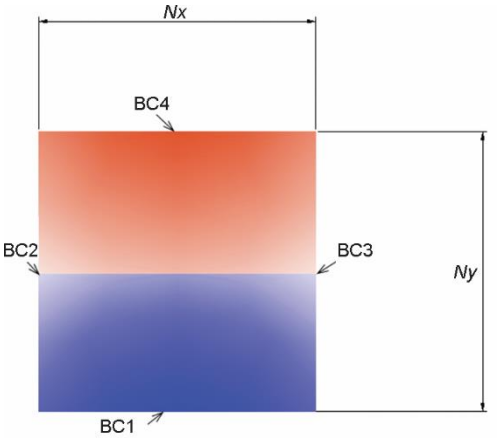

Figure 1. Set-up of the binary diffusion case

$$\rho_\sigma(y) = \frac{1}{2}\left[(\rho_{\sigma,h} + \rho_{\sigma,l}) + (\rho_{\sigma,h} - \rho_{\sigma,l}) \tan\left(\frac{y - \frac{1}{2} y_{max}}{\delta_{th}} \right) \right] \tag{33}$$

$$\rho_\varsigma(y) = \frac{1}{2}\left[(\rho_{\varsigma,h} + \rho_{\varsigma,l}) + (\rho_{\varsigma,h} - \rho_{\varsigma,l}) \tan\left(\frac{y - \frac{1}{2} y_{max}}{\delta_{th}} \right) \right] \tag{34}$$

where y_{max} is the domain length and δ_{th} is the thickness of the diffusion profile. For this computation, δ_{th} = 0.1 mm. The minimum and maximum densities are $\rho_{\sigma,h} = \rho_{\varsigma,h} = 1.123$ kg/m^2 and $\rho_{\sigma,l} = ho_{\varsigma,l} = 0.07$ kg/m^2, respectively.

The second study is that of two gases with different molecular weights diffusing into each other. Here convection is not considered and reactions are neglected. The binary diffusion coefficients $D_{\sigma c}$ = 0.68 cm^2/s, the computational domain has 500 lattice nodes in the y-direction and boundary conditions are the same as in the previous study. The lattice spacing is $(2\delta_t)^{1/2}$ with δ_x = 2 um and δ_t = 3 ns. The initial gas density for each species follows eqs. (33) and (34) with δ_{th} = 0.05 mm, $\rho_{\sigma h}$ = 1.250 kg/m^2, $\rho_{c.h}$ = 0.625 kg/m^2, $\rho_{\sigma l}$ = 0.0007 kg/m^2, and $\rho_{c.l}$ = 0.00035 kg/m^2.

Case 2. Counter-current propane/air reacting flow

Model and assumptions

In this section, a counter-flow premixed flame is modeled for simulation of combustion field. The 2-D rectangular coordinates are used. Two parallel stationary walls are located at $y = -L$ and L, where L is the half-length of the distance between walls. The combustible mixture is uniformly injected from the top and bottom walls, and it reacts in the reaction zone. Then, two reaction fronts are formed in this flow. The burned gas flows outward along the x-direction.

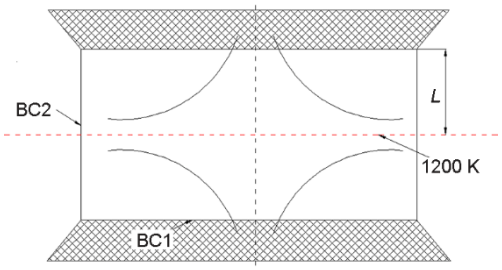

Figure 2. Schematics of this flame formed in counter flow

Figure 2 shows the schematics of this flame formed in counter flow. The fuel is propane and it is premixed with air. The reaction is an over-all one step reaction, expressed:

$$C_3H_8 + 5O_2 \rightarrow 4H_2O + 3CO_2 + \dot{Q} \quad (35)$$

where $\dot{Q}$ is the heat of overall reaction. The overall reaction rate ω_{ov} is calculated by the Arrhenius law:

$$\omega_{\text{ov}} = k_{\text{ov}} C_{C_3H_8} C_{O_2} \exp\left(-\frac{E}{RT}\right) \quad (36)$$

with $C_{C_3H_8}$ and C_{O_2} are molar concentrations for species C_3H_8 and O_2, k_{ov} – the reaction coefficient, and E – the effective activation energy. To obtain the reaction rate, the molar concentration of propane or oxygen is determined by:

$$C_k = \frac{\rho_0 Y_k}{M_k}\left(\frac{T_0}{T}\right) \quad (37)$$

where M_k is the molecular weight of species k, Y_k, is the mass fraction of species k. The mass rate of production for species k can de computed as:

$$\omega_k = a_k M_k \omega_{\text{ov}} \quad (38)$$

where a_k are the stoichiometric coefficients. In this reaction, $a_{C_3H_8} = -1$, $a_{O_2} = -5$, $a_{CO_2} = 3$ $a_{CO_2} = 3$, $a_{H_2O} = 4$.

Based on Yamamoto's study [33], the following assumptions are made: Nitrogen is assumed to be inert, there are no external forces; viscous energy dissipation and radiative heat loss are neglected, and thermo-compression is not taken account.

Boundary conditions and parameters

The length of the distance between walls is 20 mm, and longitude length is 33.4 mm. The number of grids is 301 × 181, and the mesh size is about 0.05 mm. We prescribe the following boundary conditions:

The BC1-inlet: At the top and bottom walls, the inflow boundary is constant velocity boundary condition for flow, and hydrodynamic condition for temperature and concentration. The velocity, $U_0 = 0.2$ m/s, temperature, T_0, is room temperature ($T = 300$ K), and concentration are those of unburned mixture. We assume constant mass fraction $Y_{C_3H_8,in} = 0.037$, $Y_{O_2,in} = 0.2245$ and $Y_{N_2,in} = 0.7385$.

The BC2-outlet: At the left and right sides of the reaction zone, we assume zero-gradient boundary condition.

$$f_k(\vec{x}) = f_k(\vec{x} - \delta_x) \tag{39}$$

The simulation starts with the initial conditions: $u = 0$, $Y_k = Y_{k.in}$ for all species; $T_0 = 300$ K for everywhere except the center, $T_{center} = T = 1200$ K, $\rho_0 = 1$.

In LB model the non-dimensional inlet velocity and density are 0.1 and 1, respectively. Other parameters used in the calculation are shown in tab. 1 [33]:

Table 1. Parameters used in counter-current propane/air reacting flow case

k_{ov}	$9.9 \cdot 1013$ (cm^3/mols)
E	30 kcal/mol
v	$1.6 \cdot 10^{-5}$ m^2/s
Q	$2.05 \cdot 10^6$ J/mol
k	$2.2 \cdot 10^{-5}$ m^2/s
C_p	$1.01 \cdot 10^3$ J/kgK

Numerical results and discussion

Case 1. Binary diffusion flow

In this case, the model is tested for binary diffusion problems, the LB method results are compared to computations from [32]. The multi-component Boltzmann equation in the reference includes multiple collision terms accounting for inter-species interaction, using appropriate relaxation parameters, this model is shown to reproduce the Maxwell-Stefan equation for species diffusion. The equations are spatially discretized with a second-order central-difference scheme and temporally with a first-order scheme. In present model, binary Maxwell-Stefan diffusivities can be calculated by:

$$D_{i,j} = D_1(i,j) + D_2(i,j)n_{i+j} \tag{40}$$

where $D_1(i, j)$ and $D_2(i, j)$ are species-dependent coefficients and n_{i+j} denotes the combined number density of species i and j. Figure 3 shows the density profile of each species at $t = 0$ ms, 0.044 ms, 0.088 ms, and 0.0176 ms, the results from the LB model and the reference compare well and the error is less than 1% at all locations and times. Therefore, this model was shown to reproduce the correct macroscopic hydrodynamic equations.

Then we simulate two gases with a molecular weight ratio of 2 diffusing into each other. Figure 4 shows the density profile for each species at $t = 0$ ms, 0.02 ms, 0.05 ms, and 0.1 ms for both the reference and present computations. The results compare well with less than 1% error at all locations and times.

Case 2. Counter-current propane/air reacting flow

First, we show the flow field where counter-current reacting flow flames are formed. Pressure waves appear in the numerical domain at the beginning of the simulation. In order to get a steady-state solution, the simulation must be pursued for many iterations. Figure 5

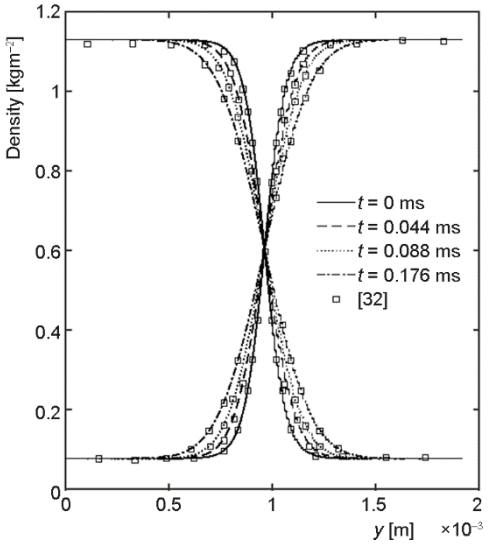

Figure 3. Binary mixture diffusion results at different times compared to data taken from [32]

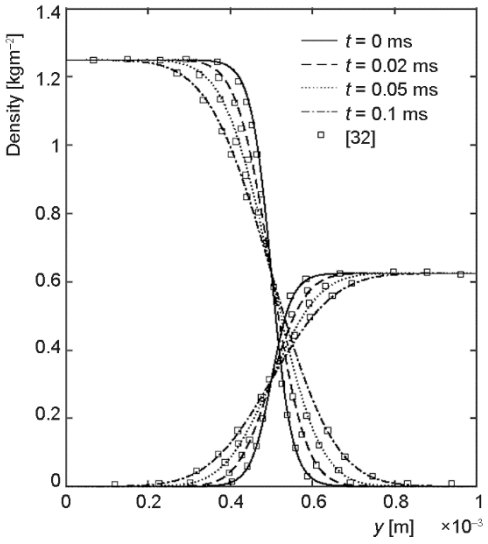

Figure 4. Density profile for binary diffusion of two species with molecular weight ratio of 2/1 at different times compared to data from [32]

shows the distribution of velocities of v_x at $y = L_y/2$ and v_y at $x = L_x/2$, respectively. The velocity is normalized to the inlet velocity at the wall, U_0. The velocity profile agrees very well with the results obtained by Yamamoto's model [33] and the results of Hosseini *et al.* [34]. The flow field is well simulated in the case of counter flow. Yamamoto *et al.* [33] solved the advection diffusion equation only for the species involved in the reaction and the Fick approximation were absorbed into the diluting species. In [34], a modified model taking account the correction velocity was run in order to clarify the effect of each modification onto the original advection diffusion scheme. In our study, a finite discrete velocity model is derived to solve the flow field. Under the assumption of a diluted flame, the results are perfectly matched.

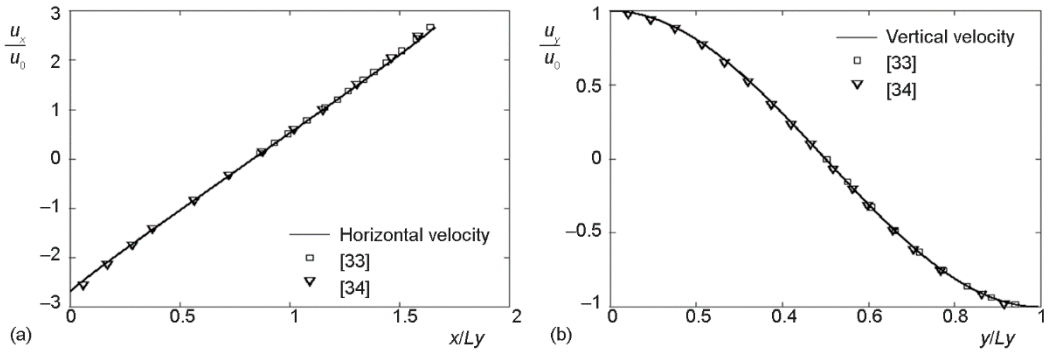

Figure 5. Distributions of non-dimensional velocities: (a) *x*-component along vertical centerline and (b) *y*-component along horizontal centerline compared to data from [34]

Next, we examine the flame temperature. As seen in fig. 6, the maximum temperature is almost constant. As the center is approached, the temperature starts to increase at

y/Ly = 0.6, and steeply increases at y/Ly = 0.6-0.7. The reaction zone located in this region, where the large heat release occurs to cause the temperature increase. Then, temperature becomes constant in the burned gas region. The results obtained are agreement with the data from [33, 34]. This agreement was expected as all thermochemical properties employed in this case are fixed and homogeneous in space, therefore, they do not depend on local composition or temperature. Additionally, the flame is diluted, reducing the importance of density gradients and molecular diffusion.

Figure 7 shows the mass fraction profiles when the reactive flow achieves the steady state. As seen in this figure, the reactants, C_3H_8 and O_2, begin decreasing at the edge of preheat zone, and react in the reaction zone to form the products, CO_2 and H_2O. Figure 8 compare these results with those by Yamamoto *et al.* [33] and Hosseini *et al.* [34]. We see that the distributions of mass fraction profiles are matched.

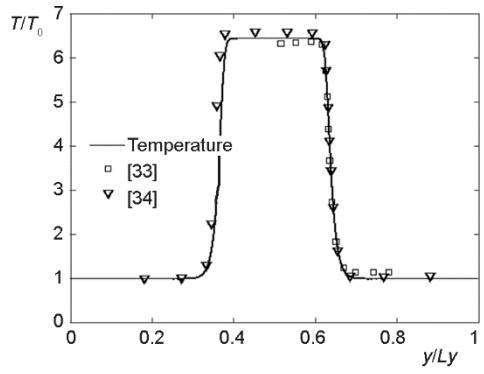

Figure 6. Distributions of non-dimensional temperature along vertical centerline compared to reference data from [33, 34]

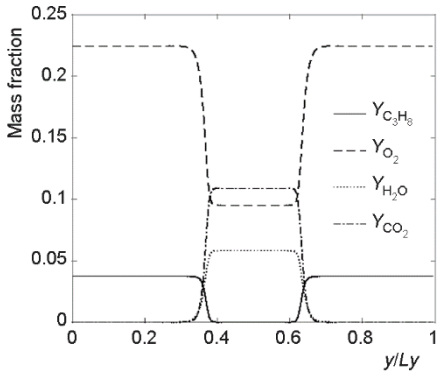

Figure 7. Mass fraction of species along vertical centerline

The overall structure of the velocity field along with the velocity profile on the vertical centerline is represented in fig. 9. As shown in fig. 10, the fine structure of counter-flow flame is observed. At the flame stagnation position, the reaction rate reaches its peak value.

Conclusion

In the context of the present study, a developed LB code for multi-species reacting flows was analyzed. A fully discrete LB scheme is derived by integration along the characteristics. The binary diffusion cases demonstrated the capabilities of the model and its boundary conditions. The performance of this model is excellent and maintain the computational advantages of the standard LB method. An propane/air reacting flow involving five species has been computed with the resulting solver, the LB results show excellent agreement compared to a classical reference solution obtained by finite differences. The next step would be to extend it to fully dilatable flows. Error terms in both the flow field and passive scalar transport equations would have to be taken account.

Acknowledgment

Thanks to my supervisors, Dr. Seyed Ali Hosseini and Prof. Dr. Dominique Thévenin of the Institute of Fluid Dynamics and Thermodynamics at the University of Magdeburg. This work was supported by the project of National Key R&D Program of China (No.

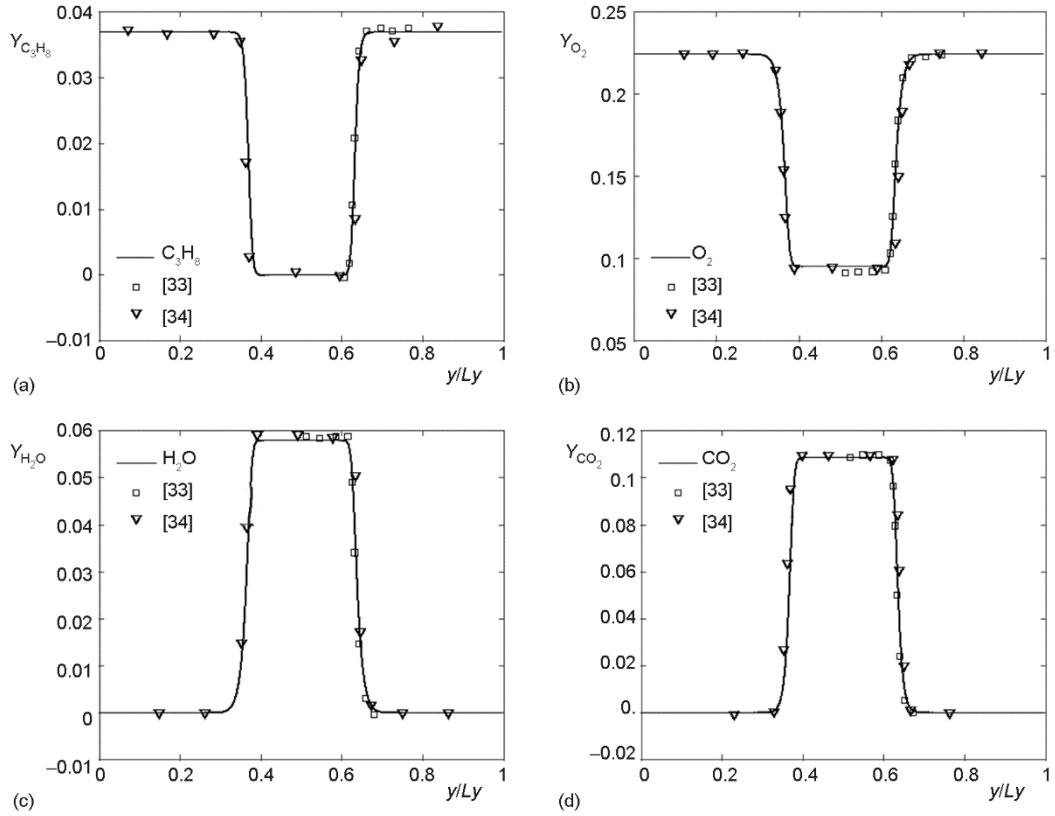

Figure 8. Distributions of mass fraction along vertical centerline for; (a) C_3H_8 (b) O_2 (c) H_2O, and (d) CO_2 compared with data from [33, 34]

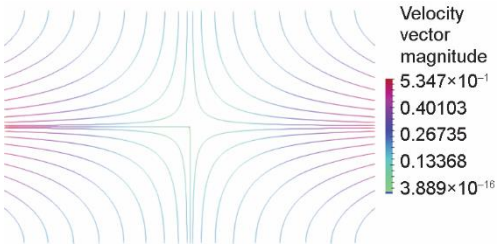

Figure 9. Overall flow structure for the propane/air configuration: streamlines

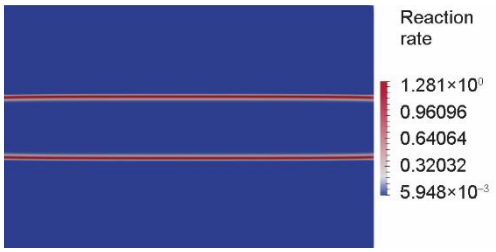

Figure 10. Reaction rate for the counter-flow propane/air configuration

2018YFB0606101), the General Program of National Natural Science Foundation of China (No. 51779107), the National Natural Science Foundation of China (No. 51809120), the Natural Science Foundation of Jiangsu Province (No. BK20180871), the Project Funded by China Postdoctoral Science Foundation (No. 2018M640462) and the Natural Science Foundation of the Jiangsu Higher Education Institutions of China (No. 18KJB470005).

References

[1] Yin, X. W., Zhang, J. F., An Improved Bounce-Back Scheme for Complex Boundary Conditions in Lattice Boltzmann Method, *Journal of Computational Physics, 231* (2012), 11, pp. 4295-4303
[2] Aidun, C. K., Clausen J. R., Lattice-Boltzmann Method for Complex Flows, *Annual Review of Fluid Mechanics, 42* (2010), 1, pp. 439-472
[3] Bhatnagarand, P. L., *et al.*, A Model for Collision Processes in Gases. I. Small Amplitude Processes in Charged and Neutral One-Component Systems, *Physical Review*, *94* (1954), 3, pp. 511-525
[4] Bao, Y. B., Meskas, J., *Lattice Boltzmann method for fluid simulations,* Department of Mathematics, Courant Institute of Mathematical Sciences, New York University, N. Y., USA, 2011
[5] Hou, S. L., *et al.*, Simulation of Cavity Flow by the Lattice Boltzmann Method, *Journal of Computational Physics, 118* (1995), 2, pp. 329-347
[6] Gunstensen, A. K., *et al.,* Lattice Boltzmann Model of Immiscible Fluids, *Physical Review A, 43* (1991), 8, 4320
[7] Orlandini, E., *et al.*, A Lattice Boltzmann Model of Binary-Fluid Mixtures, *Europhysics Letters, 32* (1995), 6, 463
[8] Osborn, W. R., *et al.*, Lattice Boltzmann Study of Hydrodynamic Spinodal Decomposition, *Physical review letters, 75* (1995), 22, 4031
[9] Swift, M. R., *et al.*, Lattice Boltzmann Simulations of Liquid-Gas and Binary Fluid Systems, *Physical Review E, 54* (1996), 5, 5041
[10] Sofonea, V., Sekerka, R. F., BGK Models for Diffusion in Isothermal Binary Fluid Systems, *Physica A: Statistical Mechanics and its Applications, 299* (2001), 3, 494
[11] Filippova, O., Hanel, D., Lattice-BGK Model for Low Mach Number Combustion, *International Journal of Modern Physics C, 9* (1998), 8, 1439
[12] Filippova, O., Hanel, D., A Novel Lattice BGK Approach for Low Mach Number Combustion, *Journal of Computational Physics, 158* (2000), 2, pp. 139-160
[13] Andries, P., *et al.*, A Consistent BGK-Type Model for Gas Mixtures, J*ournal of Statistical Physics, 106*(2002), 5, pp. 993-1018
[14] Sirovich, L. , Kinetic Modeling of Gas Mixtures, *The Physics of Fluids, 5* (1962), 8, pp. 908-918
[15] Luo, L. S., Girimaji, S. S., Lattice Boltzmann Model for Binary Mixtures, *Physical Review E, 66* (2002), 3, 035301
[16] Xu, A. G., Two-Dimensional Finite-Difference Lattice Boltzmann Method for the Complete Navier Stokes Equations of Binary Fluids, *Europhysics Letters, 69* (2004), 2, 214
[17] Asinari, P., Viscous Coupling Based Lattice Boltzmann Model for Binary Mixtures, *Physics of Fluids, 17* (2005), 6, 067102
[18] Asinari, P., Semi-Implicit-Linearized Multiple-Relaxation-Time Formulation of Lattice Boltzmann Schemes for Mixture Modeling, *Physical Review E, 73* (2006), 5, 056705
[19] Arcidiacono, S., *et al.,* Lattice Boltzmann Model for the Simulation of Multicomponent Mixtures, *Physical Review E, 76* (2007), 4, 046703
[20] Flekkoy, E. G., Lattice Bhatnagar-Gross-Krook Models for Miscible Fluids, *Physical review. E, Statistical physics, plasmas, fluids, and related interdisciplinary topics, 47* (1993), 6, pp. 4247-4257
[21] Shan, X. W., Chen, H. D., Lattice Boltzmann Model for Simulating Flows with Multiple Phases and Components, *Physical Review E, 47* (1993), 3, pp. 1815-1819
[22] Shan, X. W., Chen, H. D., Simulation of Nonideal Gases and Liquid-Gas Phase Transitions by the Lattice Boltzmann Equation, *Physical Review E, 49* (1994), 4, 2941
[23] Zhang, R. Y., Chen, H. D., Lattice Boltzmann Method for Simulations of Liquid-Vapor Thermal Flows, *Physical Review E*, *67* (2003), 6, 066711
[24] Li, Q., *et al.*, Lattice Boltzmann modeling of Boiling Heat Transfer: The Boiling Curve and the Effects of Wettability, *International Journal of Heat and Mass Transfer*, *85* (2015), June, pp. 787-796
[25] Zheng, S. F., *et al.*, Numerical Investigation of Convective Dropwise Condensation Flow by a Hybrid Thermal Lattice Boltzmann Method, *Applied Thermal Engineering*, *145* (2018), Dec., pp. 590-602
[26] Zheng, S. F., *et al.*, Single Droplet Condensation in Presence of Noncondensable Gas by a Multi-Component Multi-Phase Thermal Lattice Boltzmann Model, *International Journal of Heat and Mass Transfer, 139* (2019), Aug., pp. 254-268
[27] Zudrop, J., *et al.*, A Robust Lattice Boltzmann Method for Parallel Simulations of Multicomponent Flows in Complex Geometries, *Computers & Fluids, 153* (2017), Aug., pp. 20-33

[28] Eshghinejadfard, A., Thevenin, D., Numerical Simulation of Heat Transfer in Particulate Flows using a Thermal Immersed Boundary Lattice Boltzmann Method, *International Journal of Heat & Fluid Flow, 60* (2016), Aug., pp. 31-46
[29] Eshghinejadfard, A., *et al.*, Direct-Forcing Immersed Boundary Lattice Boltzmann Simulation of Particle/Fluid Interactions for Spherical and Non-Spherical Particles, *Particuology, 25* (2016), Apr., pp. 93-103
[30] Poinsot, T., Veynante, D., *Theoretical and Numerical Combustion*, 2nd ed., R. T. Edwards, London, UK, 2005
[31] Ning, C., Modeling Reacting Multi-Species Flows with a Multi-Fluid Lattice Boltzmann Scheme, M. Sc. thesis, University of Magdeburg, Magdeburg, Germany, 2018
[32] McCracken, M. E., Abraham, J., Lattice Boltzmann Methods for Binary Mixtures with Different Molecular Weights, *Physical Review E, 71* (2005), 4, 046704
[33] Yamamoto, K., *et al.*, Simulation of Combustion Field with Lattice Boltzmann Method, *Journal of statistical physics, 107* (2002), 1-2, pp. 367-383
[34] Hosseini, S. A., *et al.*, Mass-Conserving Advection Diffusion Lattice Boltzmann Model for Multi-Species Reacting Flows, *Physica A: Statistical Mechanics and its Applications, 499* (2018), June, pp. 40-57

Paper submitted: June 26, 2019
Paper revised: March 2, 2020
Paper accepted: March 4, 2020